In-Situ Synchrotron WAXD/SAXS Studies of Structural Development during PBO/PPA Solution Spinning

Shaofeng Ran,[†] Christian Burger,[†] Dufei Fang,[†] Xinhua Zong,[†] Sharon Cruz,[†] Benjamin Chu,*[,†] Benjamin S. Hsiao,*[,†] Robert A. Bubeck,[‡] Kazuyuki Yabuki,[§] Yoshihiko Teramoto,[§] David C. Martin,[⊥] Michael A. Johnson,[⊥] and Philip M. Cunniff[#]

Department of Chemistry, State University of New York at Stony Brook, Stony Brook, New York 11794-3400; Michigan Molecular Institute, 1910 W St Andrews Rd, Midland, Michigan 48640; Toyobo Co. Ltd., Research Center, Katata, Ohtsu, Shiga 520-0292, Japan; Department of Materials Science and Engineering, University of Michigan, Ann Arbor, Michigan 48109-2136; and Department of the U.S. Army, Soldier and Biological Chemical Command, Natick, Massachusetts 01760-5019

Received February 12, 2001; Revised Manuscript Received October 18, 2001

ABSTRACT: Combined wide-angle X-ray diffraction (WAXD) and small-angle X-ray scattering (SAXS) studies using synchrotron radiation were carried out to investigate the structural development during in-situ solution spinning of poly(*p*-phenylenebenzobisoxazole) (PBO) in poly(phosphoric acid) (PPA). WAXD patterns indicated that the structure in the extruded PBO/PPA dope before coagulation (in water) possessed lyotropic "biaxial nematic" nematic order involving PBO−PPA complex as the mesogenic unit. A different biaxial nematic order in pure PBO was found to develop immediately upon coagulation in water. When the coagulation time exceeded 30 min, the complex PBO/PPA structure completely disappeared, and well-oriented PBO crystals were formed. The meridian peaks exhibited long streaks, indicating a translational disorder of PBO molecules in the fiber direction. SAXS patterns of the PBO fiber after coagulation showed equatorial streaks with no further maxima observed, which is attributed to a microvoid structure.

Introduction

High-modulus and high-strength fibers have been of continuous interest for research and practical applications over the past two decades. Exceptionally high tensile properties can be obtained in fully extended rigid-chain polymers such as poly(*p*-phenylenebenzobisoxazole) (PBO or PBZO). The Young's modulus of PBO fiber has been reported as high as 350 GPa,[1] which is significantly greater than that of poly(*p*-phenylene terephthalamide) (PPTA) fiber.[2] It has also been demonstrated that PBO fibers have superior thermal stability and solvent resistance than PPTA fibers.

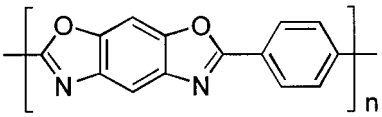

PBO is usually prepared by polymerization of 4,6-diamino-1,3-benzenediol dihydrochloride and terephthaloyl dichloride in poly(phosphoric acid) (PPA).[3−7] The resultant polymer mixtures (dope) with concentrations of approximately 5−15 wt % in PPA or other solvents are suitable for dry-jet wet spinning, which can produce high-modulus and high-strength fibers.[3,5,8,9] Although the as-prepared PBO/PPA dope is often thought to possess some sort of lyotropic order, the nature of the structure in the dope (such as lyotropic liquid crystal or three-dimensional (3D) crystal complex) is still unclear. For example, when the dope is extruded from the spinneret (at high temperatures) under certain shear rates, it has been reported that the extrudate exhibits a liquid crystalline structure with a high degree of molecular orientation.[10]

During spinning, the oriented structure of the extrudate can be transformed into the crystalline phase by coagulation in water in many sequential events. For example, after full coagulation (all PPA contents are washed away by water) and drying, the PBO fiber is referred as the AS (as-spun) fiber. The AS fiber strength can be enhanced by subsequent heat treatments under tension, which result in HM (high-modulus) fibers.[3,9,10,11] The properties of AS fibers are highly dependent on the spinning conditions,[3,8] as the varying processing conditions can produce different structure and morphology. In the present study, we are interested in understanding the structure and morphology development during spinning, particularly prior to and during the coagulation process.

To understand the intermediate structure during spinning, prior knowledge about the PBO crystal structure is essential. The PBO crystal structure has been studied quite extensively over the past two decades using different methods.[12−25] It has been determined that PBO chains crystallize into a monoclinic unit cell with parameters $a = 11.20$ Å, $b = 3.5$ Å, $c = 12.0$ Å, and $\gamma = 101.3°$,[17] where the *c*-axis represents the chain axis. In the crystal structure, the neighboring chains exhibit axial shifts of $+c/4$ or $-c/4$ distance.[16,25] In addition, a translational disorder along the chain axis can cause distinct streaking in the layer lines of the X-ray diffraction patterns.[1,16,20] Several groups have considered this translational disorder in the analysis of the diffraction data.[26,27] It has been noted that the aromatic rings can be twisted, producing another kind

[†] State University of New York at Stony Brook.
[‡] Michigan Molecular Institute.
[§] Toyobo Co. Ltd.
[⊥] University of Michigan.
[#] Soldier and Biological Chemical Command.
* To whom correspondence should be addressed. E-mail bchu@notes.cc.sunysb.edu or bhsiao@notes.cc.sunysb.edu.

10.1021/ma010249g CCC: $22.00
Published on Web 12/13/2001

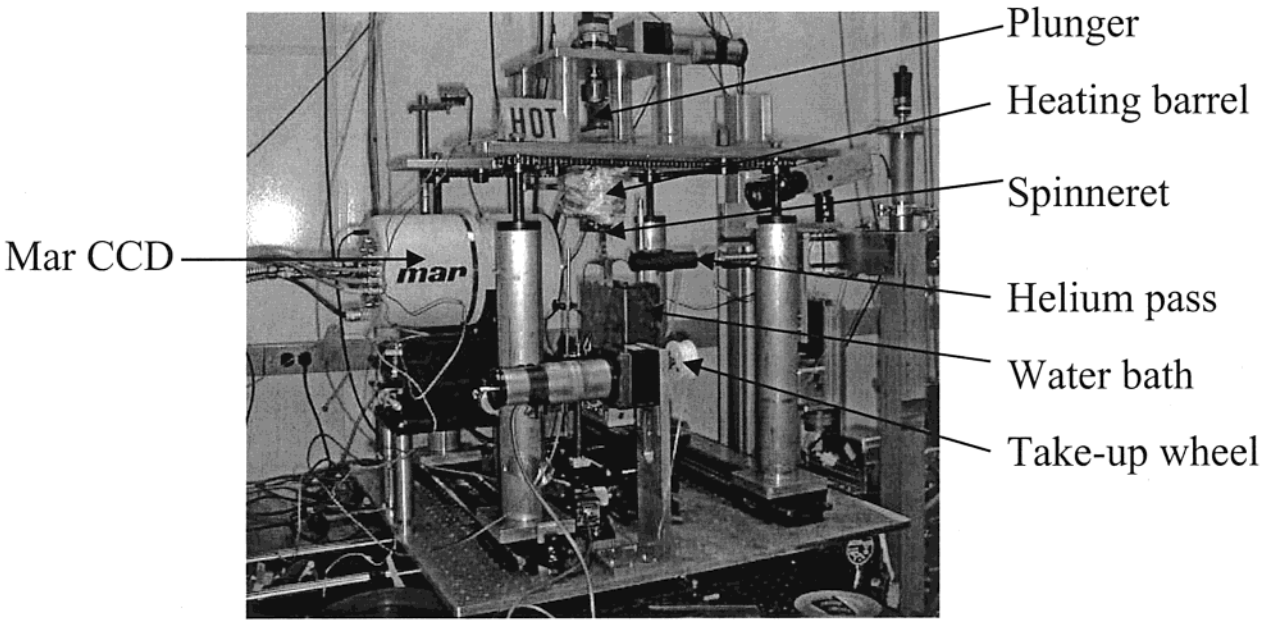

Figure 1. Photograph of the PBO in-situ spinning apparatus with MAR CCD detector at the beamline X27C in NSLS, BNL.

of defect in the crystal structure.[25] It is not clear, however, if these are point defects (single chain twists) or are cooperative twists of adjacent chains. Both twists are possible. The microstructure of PBO crystals has been studied by TEM,[14−16] which provided direct evidence of the high degree of local orientation as well as lateral packing in the crystallized polymer chains.

In the PBO fiber, the rigid chains are aligned parallel to the fiber axis.[13] On the basis of the literature,[14,16,28] "crystallite sizes" in the PBO fiber in the range of 100−200 Å have been reported (in both fiber and transverse directions), although not much details for the nature of these crystallites and their surroundings have been provided. In terms of the intermediate structures staged between the initial dope and the final crystal, Cohen et al. reported several interesting crystal-solvate phases in PBO and PBZT (poly[*p*-phenylene(benzo[1,2-*d*:4,5-*d*′]-bisthiazole-2,6-diyl)]).[29−32] They found that, under different equilibrium conditions, the undeformed polymer (PBO and PBZT) can complex with different compositions of PPA solvent and water coagulant to form different phases. Unfortunately, the unit cells given by Cohen et al. are very large, and no information about their contents was provided. It has also been reported that when the PBO fiber was heat-treated between 500 and 700 °C in N_2 for a short period of time,[13,33−35] a four-point pattern in SAXS was seen.[28,35] Detailed analysis and interpretation of the four-point pattern in SAXS have been made by Kumar et al.[35] and later by Yabuki et al.[28] In-situ structural studies during PBO fiber spinning were carried out previously by scientists from Dow Chemical Company using synchrotron wide-angle X-ray diffraction (WAXD).[10,36,37] From their work, the effects of line tension, spin draw ratio (SDR), and temperature on the orientation parameter and the microdomain size before the coagulation process were examined.

It is clear that many open questions remained in solution spinning of PBO in PPA. For example, how many stages in the evolution of the microstructure can occur, starting from the extruded lyotropic solution and ending with the fully coagulated AS fiber? What is the nature of the "crystal phase" or the "liquid crystal phase" during the different stages of the process, and how should they be correlated with their surroundings? To answer some of these questions, we have carried out an in-situ PBO monofilament dry-jet wet spinning study using the combined methods of WAXD and SAXS with synchrotron radiation.

Experimental Section

The fiber spinning apparatus used in this study was a modified version of the experimental setup constructed by Dow scientists.[10,37] A photograph of this modified apparatus used for the in-situ WAXD experiment is shown in Figure 1. A capillary rheometer-like barrel was located on the top platform of this apparatus, which stored the polymer solution with upper temperature capability of 300 °C. A motor-driven plunger was used to extrude the polymer solution. The top platform could be moved vertically over a distance of about 10 cm with a 0.2 mm precision, allowing the detection spot along the spin line to be changed. The apparatus was mounted on a pair of precision optical rails perpendicular to the X-ray beam, which permitted the alignment of the monofilament fiber with the X-ray beam. A take-up wheel with adjustable speed provided the means to change the spin draw ratio (SDR), which is defined as the ratio of the fiber take-up speed to the extrudate speed at the spinneret exit. A water bath was installed for studying the coagulation process. With an integrated system of fine position control and X-ray beam monitor, the detection spot on the filament could be quickly switched before and after coagulation. A helium gas flow chamber was placed between the last pinhole and the filament to minimize the air scattering. The PBO/PPA dope (about 14 wt % of PBO) was sealed in custom-made PVC pipes fitted with Teflon caps, which were provided directly by Toyobo Inc., Japan. To eliminate any possibility of moisture contamination in the dope, these airtight PVC pipes (containing the dope) were further enclosed in sealed plastic bags, which were stored in a drybox filled with nitrogen and covered by black papers. During the experiment, the barrel was first heated to the spinning temperature (160 °C). The dope was removed by cutting open the PVC tube, which was exposed to the atmosphere for an average of 3 s. The spinning was carried out using the extrusion speed of ∼10 mm/s. The exit opening of the spinneret was 0.75 mm in diameter.

The spinning experiment was carried out in the Advanced Polymers Beamline X27C at the National Synchrotron Light Source (NSLS), Brookhaven National Laboratory (BNL). This

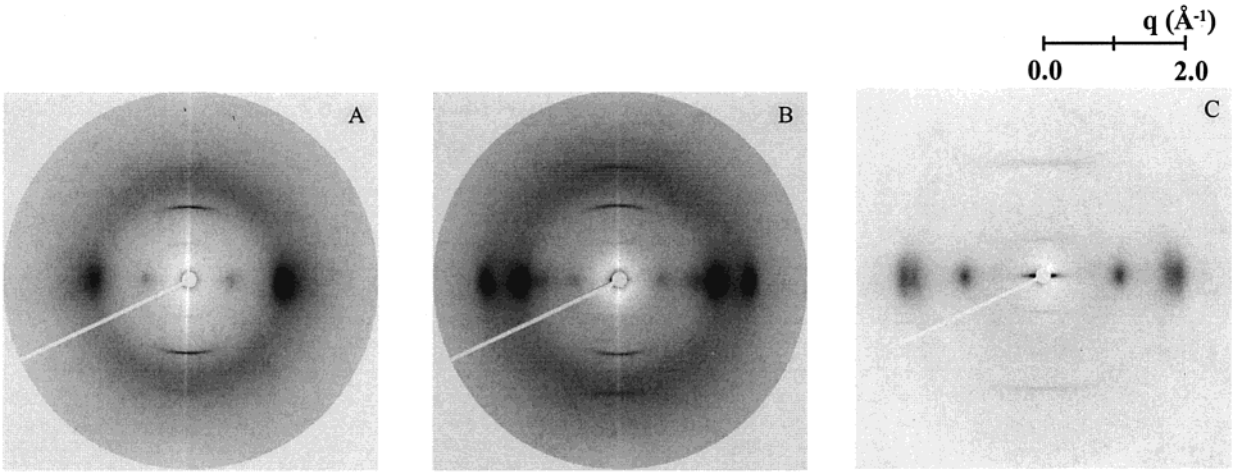

Figure 2. 2D raw WAXD patterns of PBO fiber with SDR of 10.0, bath temperature of 60 °C at different stages: (A) before coagulation, (B) 2 s of coagulation (under tension), (C) 30 min of coagulation (no tension).

beamline consists of a high-precision pinhole system that is suitable for SAXS/WAXD studies. The X-ray beam ($\lambda = 0.137$ nm) was collimated though a three-pinhole system (190 cm long) with the last pinhole size being 0.37 mm in diameter. Using a custom-designed X-ray beam spot monitoring system, the synchrotron beam was easily aligned with the fiber having a diameter of about 50 μm. Each image from the moving fiber was exposed to the X-ray beam for about 2 min. Separate two-dimensional (2D) WAXD and SAXS patterns were recorded by using a CCD X-ray detector (MAR-USA). The distance between the detector and the sample for WAXD was 112.9 mm, which was calibrated using an Al_2O_3 standard. For SAXS, the distance between the detector and the sample was 1437.5 mm. For both SAXS and WAXD studies, a PIN-diode beam stop was used.[38] The reading from the PIN-diode not only provided the reference for the sample absorption correction and beam fluctuations but also offered a convenient way to verify the alignment between the fiber and the X-ray beam (note that PPA was a very strong X-ray absorber).

Results and Discussion

Structure of Uncoagulated Dope Extrudate. Typical 2D WAXD patterns (corrected for air scattering and beam fluctuations) of a PBO monofilament collected at different stages of spinning and coagulation conditions under a spin draw ratio (SDR) of 10.0 and a coagulation temperature of 60 °C are shown in Figure 2. It is seen that in the uncoagulated fiber (Figure 2A) the WAXD pattern exhibits distinct reflection arcs along the meridian, which comes from the basic repeat distance of 12 Å along the chain axis. This distance remains about constant in all the patterns observed. The most interesting observation is that a weak but distinct reflection peak at $q = 0.65$ Å^{-1} ($d = 2\pi/q = 9.67$ Å) and a broad, intense reflection peak around $q = 1.41$ Å^{-1} ($d = 4.45$ Å) on the equator are seen.

From the position ratio and the intensity difference of these two peaks, we can exclude the possibility that the structural units of this state have adopted a long-range hexagonal packing or a short-range nematic packing with isotropic cross section. In either case, the first peak would be the strongest and the peak ratio would be different (for example, 1:$\sqrt{3}$ is expected in the hexagonal structure). This is not seen in Figure 2A.

From the observed WAXD pattern, it is clear that the structure of the uncoagulated dope extrudate consists of an oriented liquid-crystalline characteristics with short-range order in the cross section. However, because of the equatorial peak positions and intensities, two incommensurable spacings in the lateral packing are present, suggesting that an anisotropic cross-section in the structural unit exits. This adds another level of anisotropic short-range order perpendicular to the order characteristic for the nematic phase. This structure fits the definition of a "biaxial nematic" phase, where the mesogenic unit is "planklike" or "boardlike".[40] In the oriented biaxial nematic phase, rotational freedom of the molecules is hindered, and two different transversal spacings are present, resulting in two distinct equatorial maxima. The solvent molecules can be intercalated between the planklike molecules.

From the PBO structure, the rigid aromatic moiety has a plank-shape geometry. Unfortunately, the two observed lateral spacings ($d = 9.67$ Å and $d = 4.45$ Å) are too large to be accounted for by a packing of PBO chains. This suggests that the plank-shaped structural unit in the oriented uncoagulated dope is larger than the single PBO chain, and the PPA molecules must be involved. It is reasonable to assume that the structural unit is a rigid, well-defined complex between PPO and PPA molecules.

In this context, it is interesting to note that Cohen et al.[29−32] have also observed equatorial peaks at 9.18 and 4.58 Å and some other positions in a crystalline PBO−PPA solvate of unknown stoichiometry. It is conceivable that in the lyotropic melt the observed two broad peaks close to these two peak positions persist. This suggests that the plank-shaped structural unit is already present in the crystalline solvate and prevails in the biaxial nematic melt. The exact structure of this complex between PPO and PPA is unknown and could also not be determined from the Cohen data.[29]

Structure of Coagulated Fiber. In Figure 2B, it is seen that, after the filament passes through the coagulation water bath (2S of coagulation under tension), two additional peaks appear around $q = 1.15$ Å^{-1} ($d = 5.46$ Å) and $q = 1.87$ Å^{-1} ($d = 3.36$ Å), which are close to the positions of the 200 and 010 reflections in pure PBO crystals, respectively. It is found that the intensity of 010 is much higher than that of 200, which means that the periodic order corresponding to the 3.36 Å spacing is more pronounced than that of 5.46 Å, implying that the 010 ordering takes place first. This observation indicates that the first step of coagulation would be removal of PPA and formation of PBO stacks (at the

3.36 Å spacing). In addition, the intensities of all the reflections due to the PBO/PPA complex become lower in Figure 2B than those in Figure 2A. This observation indicates that, upon hydrolysis and removal of PPA, PBO chains tend to segregate and form domains of pure PBO stacks in the state of order to be discussed next. With respect to the structure of the PBO domains containing segregated chains formed during the coagulation process, there are two possibilities. (1) The PBO domain may represent another biaxial nematic phase with short-range order in the fiber cross section, in which the PBO molecules themselves constitute the mesogenic units. (2) Long-range two-dimensional ordering exists in the PBO packing leading to a structure close to the ideal PBO crystals with possible translational order.

In terms of the biaxial nematic phase (possibility 1), there are also two scenarios. One is the simple biaxial nematic structure with two lateral length scales as discussed previously (but without the PPA molecules). Second is the preferred formation of stacks of PBO molecules, possibly with graphite-like π-interactions forming a kind of asymmetric biaxial nematic phase where one of the two spacings is more pronounced than the other. In both scenarios, rotation is strongly hindered. (If rotation happens, it would rotate the whole stack.) Any remaining solvent will be located between the stacks, not intercalated into the stack. The equator in WAXD of this system thus should be dominated by a strong peak near the 010 reflection of PBO, corresponding to a graphite-like interlayer spacing of 3.36 Å. At this point, we do not have sufficient information to determine which structure is more likely in the coagulated extrudate.

In Figure 2B, the total coagulation time is less than 2 s. In this case, segregated PBO chains probably occupy only a small fraction of the filament near the filament surface with the majority of the material still being the oriented uncoagulated dope, i.e., the complex of PBO and PPA. If the coagulation time is increased to 30 min, the observed structure becomes very different, and the corresponding WAXD pattern is shown in Figure 2C. It should be mentioned here that the 30 min of coagulation was not under tension (we simply soaked the spun PBO uncoagulated filament into water at room temperatures for 30 min), but the 2 s of coagulation was under tension. In Figure 2C (30 min coagulation), there are four distinct equatorial peaks having the same positions as those reported for the PBO crystal structure. The two peaks related to the PBO/PPA complex (q = 0.65 and 1.41 Å^{-1}) completely disappear. In addition to the presence of equatorial arcs and meridional streaks, no mixed *hkl* reflections were observed in Figure 2C. It has been suggested that these features are indicative of a translational disorder in the fiber direction,[1,20,24] which is the case here. Furthermore, we observed that the peak intensity at q = 2.25 Å^{-1} was significantly increased in the dry sample when all PPA moieties were removed as compared to that in the wet sample as seen in Figure 2C.

One-dimensional slices of the equatorial profiles in Figure 2 are shown in Figure 3, in which the differences in the peak positions during different stages of coagulation can be clearly seen. In Figure 3, at the early stage of coagulation (2 s), the newly formed PBO peak at d = 3.36 Å (q = 1.87 Å^{-1}) shows no sign of separation (between the expected 010 and 2$\bar{1}$0 peaks). This indicates the presence of a biaxial nematic phase with short-range order in the cross section. Furthermore, the strong intensity differences between the two newly formed equatorial PBO peaks (q = 1.15 Å^{-1} and q = 1.87 Å^{-1}) implies that stacking of PBO molecules is the predominant ordering mechanism at this stage of structural formation. In contrast, in the fiber after 30 min of coagulation, it is seen that distinct separation of the 010 and 2$\bar{1}$0 peaks occurs, which indicates that 2-D long-range order in the cross section has formed. As no off-axis peak is observed in Figure 3C, this suggests that a translationally disordered form of the PBO structure is present, which can be explained further.

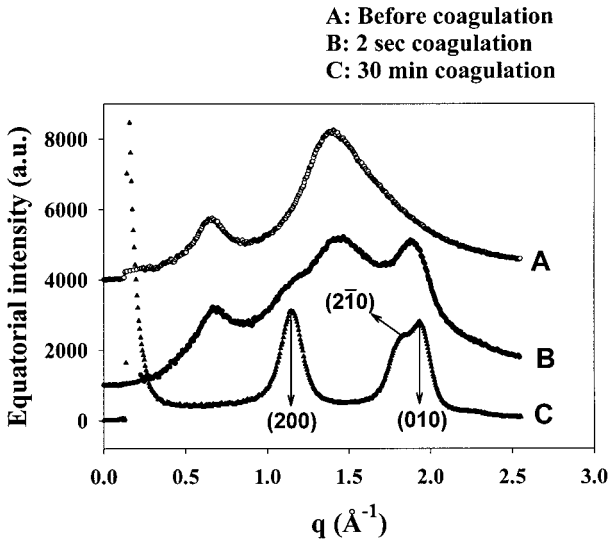

Figure 3. 1D WAXD equatorial profiles from the patterns in Figure 2.

In a fiber diffraction pattern, the absence of off-axis (mixed *hkl*) reflections indicates a translational disorder in the fiber direction of laterally packed periodic structural units. Analogue to this, the absence of mixed *hk*0 reflections (like the 2$\bar{1}$0 on the equator in Figures 2 and 3), with only *h*00 (e.g., 200) and 0*k*0 (e.g., 010) type reflections remaining, can be interpreted in terms of a 2D translational disorder in the fiber cross section. In other words, the periodic structural unit is (the cross section of) a stack of flat molecules, giving rise to a 0*h*0 type peak near the eventual 010 reflection; the translationally disordered lateral packing of (the cross section of) these stacks produces a *h*00 type reflection near the eventual 200 reflection, and no *hk*0 type peaks like the eventual 2$\bar{1}$0 should be detected. This model would produce an asymmetric peak profile of the 0*h*0 type peaks due to the radial averaging. However, this peak shape can only be observed in an idealized situation of well-ordered stacks with large stack heights. In the more realistic picture of not too perfectly ordered stacks with modest stack heights, the observed peaks become broad, higher orders are suppressed, and peak shape asymmetries become less apparent. Furthermore, the peak due to stacking (the eventual 010) is more intense than the peak due to the lateral packing of stacks (the eventual 200) since shorter stacks with polydisperse stack heights would laterally pack in a less ordered fashion; i.e., the intrastack order is higher than the interstack order. These situations describe the conditions of a "biaxial nematic" liquid-crystalline order and are in good agreement with the data of Figure 2B. When the translational disorder in the cross section disappears, a 2D lattice with a 2D unit cell and a certain

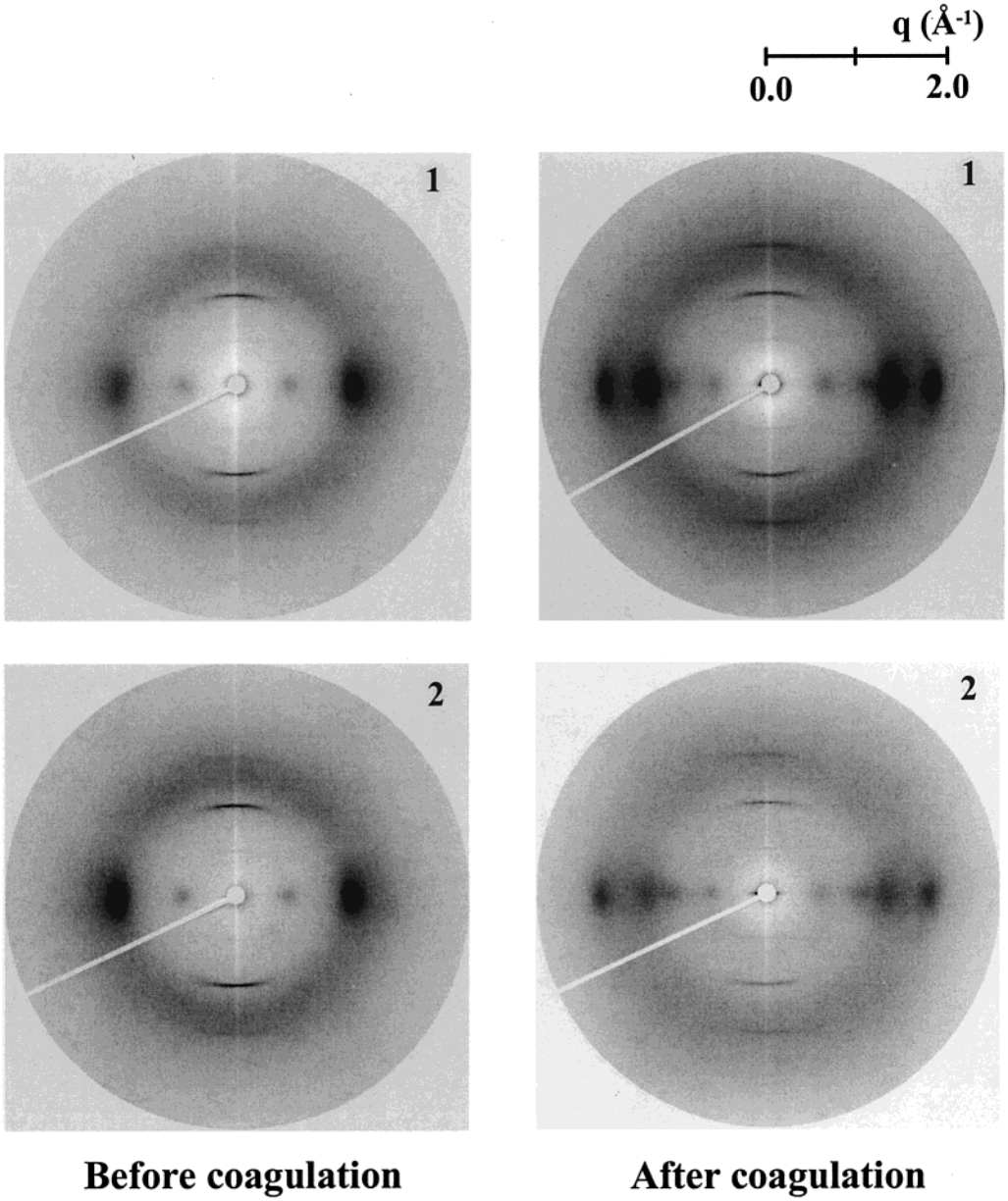

Figure 4. 2D raw WAXD patterns of PBO fiber at different spin draw ratios (SDR) before (left) and after (right) coagulation at a processing temperature of 160 °C and a bath temperature of 60 °C. SDR: (1) 5.0 and (2) 20.0.

degree of 2D long-range order has formed, and peaks corresponding to reciprocal lattice points crossing diagonals in the reciprocal lattice (like the $2\bar{1}0$) then start to appear. This is also consistent with the conditions in Figure 2C.

Effect of Deformation. Figure 4 shows the 2D WAXD patterns of the PBO filaments spun at different spin draw ratios (SDR) before coagulation and after 2 s of coagulation in a water bath (the bath temperature is 60 °C). All four patterns (raw, without the corrections of sample absorption and beam fluctuations) clearly exhibit an isotropic scattering background, which indicates the presence of an unoriented structure. The weaker intensity in pattern 2 (SDR = 20) is due to the smaller diameter filament formed at a higher draw ratio. When comparison between the corrected patterns 1 (SDR = 5) and 2 (SDR = 20) is made, the isotropic scattering background is found to decrease in the coagulated specimens with increasing SDR, which implies that the fraction of the unoriented structure is reduced. This can be attributed to the higher molecular orientation as well as more complete coagulation in the fiber. This observation indicates that the isotropic scattering background is probably dominated by the liquid PPA phase, which has been reported before.[13,17] In Figure 4, all reflections on the equator exhibit a relatively small spread along the azimuthal direction, indicating that the crystallographic *c*-axis is preferentially aligned with the fiber axis having a very high degree of preferred orientation. The spread along the azimuthal direction is found to become narrower with increasing SDR, which means that the orientation is increased with SDR.

Effect of Coagulation Temperature. 2D WAXD patterns of PBO fibers spun with SDR of 20.0 at different bath temperatures are shown in Figure 5. It is found that the bath temperature has a significant effect on the coagulation efficiency. First, the peaks become much sharper after 2 s of coagulation at the higher bath temperature (60 °C) than those at the lower bath temperature (25 °C). It has been reported that the transformation from the lyotropic liquid crystalline

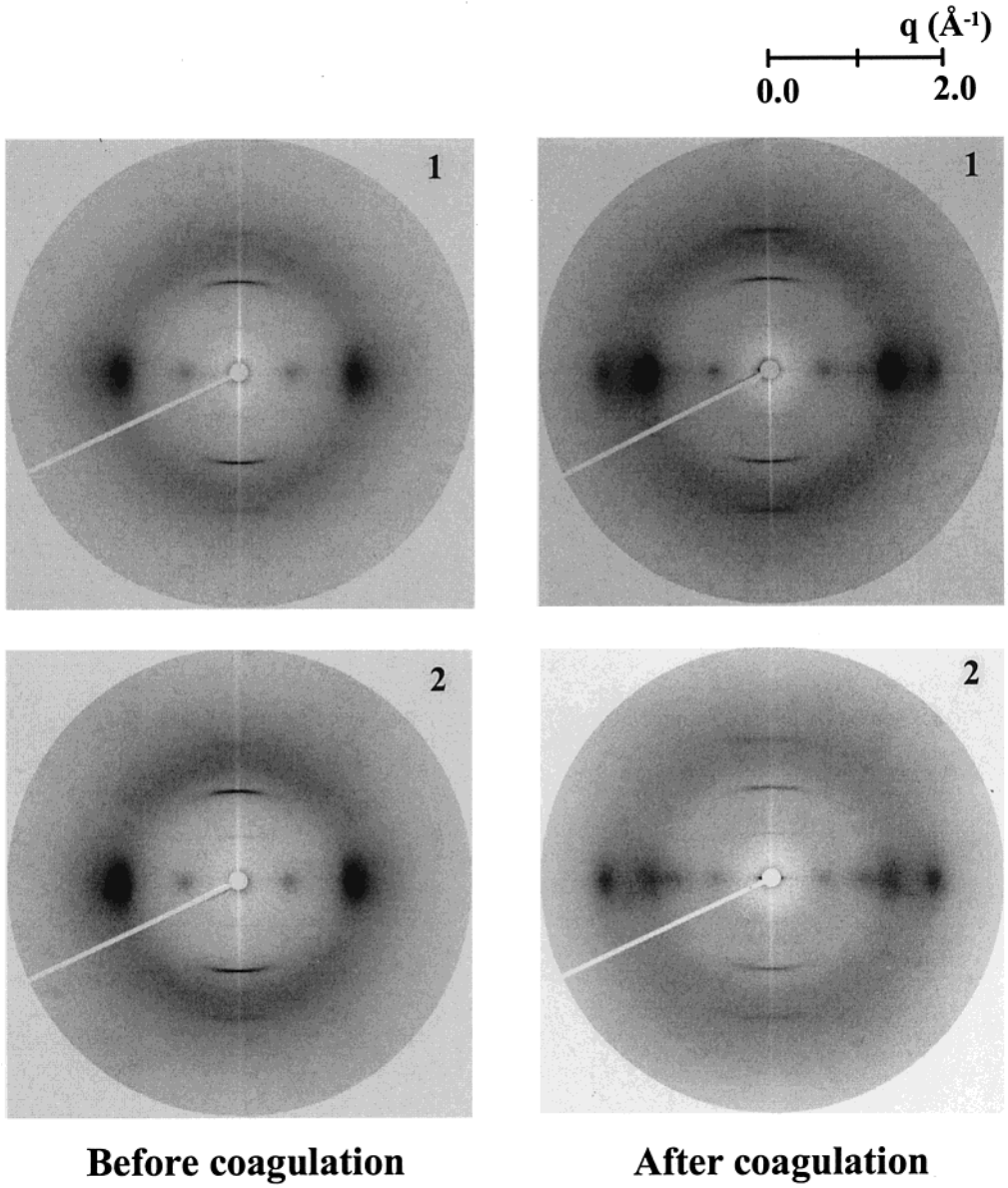

Figure 5. 2D raw WAXD patterns of PBO fiber with SDR of 20.0 before and after coagulation at a processing temperature of 160 °C. Bath temperature: (1) 25 and (2) 60 °C.

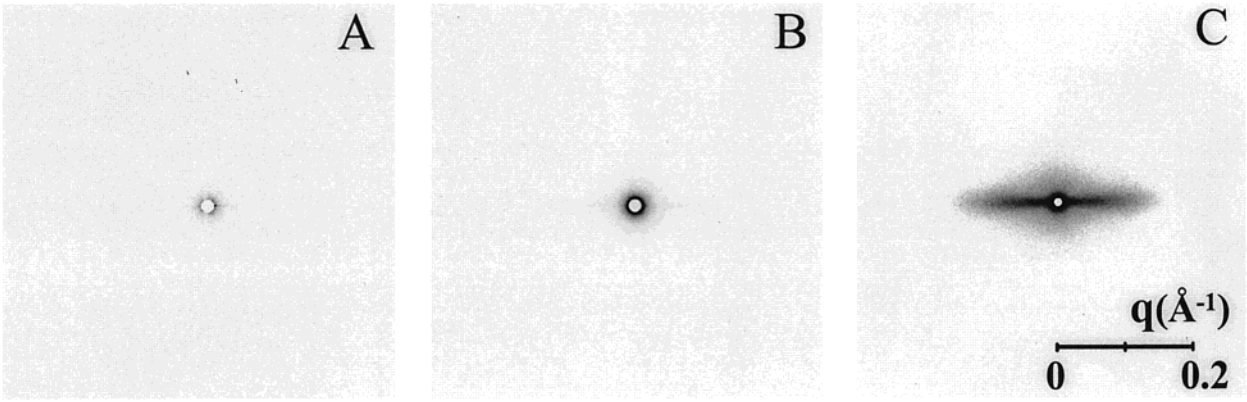

Figure 6. 2D SAXS patterns of PBO fiber with SDR of 10.0, bath temperature of 60 °C at different stages: (A) before coagulation, (B) 2 s of coagulation (under tension), (C) 30 min of coagulation (no tension).

phase to the solid-state ordered phase in PBO is mainly controlled by the diffusion process of nonsolvent water molecules during coagulation (the diffusion process could be modeled as case II diffusion).[39] The diffusion rate of the water molecule is known to increase with the increasing bath temperature. Second, the intensity of the amorphous background is found to become smaller with the increasing bath temperature, which indicates that the coagulation process is more efficient at high temperatures. However, even with the bath

temperature being 60 °C, the continued presence of the amorphous scattering background indicates that the coagulation process is far from completion after 2 s of coagulation time.

Figure 6 shows the corresponding SAXS patterns of the PBO fiber spun at a SDR of 10.0 and a coagulation temperature of 60 °C before and after coagulation. Despite the distinct structures developed by coagulation as seen in WAXD, no detectable scattering feature can be observed in the SAXS pattern of the uncoagulated filament. (The supramolecular structure in the extruded dope thus appears to be homogeneous.) Only after a short coagulation process (∼2 s of coagulation time), some intense scattering is found to develop near the beam stop. After 30 min of coagulation, the SAXS pattern shows visible equatorial streaks, which is probably due to the needle-shaped microvoids between the fibrils (having a cross-section dimension around 30 Å based on the Guinier analysis). This is consistent with the observations by Kitagawa et al., who have reported that the equatorial streak in SAXS was due to microvoids identifiable in TEM observations.[28] However, no further SAXS maxima are observed, indicating there is no additional density contrast and structural correlation in the fibrils.

Conclusions

A solution fiber spinning apparatus was used to perform in-situ structural studies during PBO spinning with synchrotron SAXS and WAXD techniques. WAXD patterns indicate that the structure before coagulation has a lyotropic liquid-crystalline order that cannot be simple nematic phase or disordered crystal phase. The best model to describe this intermediate structure is a biaxial nematic phase based on plank-shaped structural unit with PBO−PPA complex. A different type of biaxial nematic phase with PBO chains as mesogenic units was developed upon coagulation in water even in a very short period of time (∼2 s). When the coagulation time was increased (30 min), the PBO−PPA complex structure disappeared completely, and pure PBO crystals were fully formed. The meridian peaks showed streaks and no obvious off-axis reflections, indicating these crystals had translational disorder. 2D SAXS patterns of the PBO fiber after coagulation showed equatorial streaks, probably due to the presence of microvoid structures.

Acknowledgment. The financial support of this work was provided by grants from the U.S. Army Research Office (DAAG559710022, DAAD190010419, and AASERT-DAAH049510307), the Polymers Program of the National Science Foundation (DMR-9984102) and the use of the Advanced Polymers Beamline partially supported by the Department of Energy (DEFG0299-ER45760). C.B. is a Feodor Lynen Fellow. The loan of the solution spinning apparatus from the Dow Chemical Company is greatly appreciated.

References and Notes

(1) Tashiro, K.; Yoshino, J.; Kitagawa, T.; Murase, H.; Yabuki, K. *Macromolecules* **1998**, *31*, 5430.
(2) Fawaz, S. A.; Palazotto, A. N.; Wang, C. S. *Polymer* **1992**, *33*, 100.
(3) Choe, E. W.; Kim, S. N. *Macromolecules* **1981**, *14*, 920.
(4) Wolfe, J. F.; Arnold, F. E. *Macromolecules* **1981**, *14*, 909.
(5) Wolfe, J. F.; Loo, B. H.; Arnold, F. E. *Macromolecules* **1981**, *14*, 915.
(6) Cotts, D. B.; Berry, G. C. *Macromolecules* **1981**, *14*, 930.
(7) Wolfe, J. F. *Encyclopedia of Polymer Science and Technology*, 2nd ed.; John Wiley and Sons: New York, 1988; Vol. 11, pp 601−635.
(8) Hunsaker, M. E.; Price, G. E.; Bai, S. J. *Polymer* **1992**, *33*, 2128.
(9) Allen, S. R.; Filippov, A. G.; Farris, R. J.; Thomas, E. L.; Wong, C. P.; Berry, G. C.; Chenevery, E. C. *Macromolecules* **1981**, *14*, 1138.
(10) Radler, M. J.; Landes, B. G.; Nolan, D. J.; Broomall, C. F.; Chritz, T. C.; Rudolf, P. R.; Mills, M. E.; Bubeck, R. A. *J. Polym. Sci., Part B: Polym. Phys.* **1994**, *32*, 2567.
(11) Ledbetter, H. D.; Rosenberg, S.; Hurtig, C. W. *Mater. Res. Soc. Symp. Proc.* **1989**, *134*, 253.
(12) Fratini, A. V.; Adams, W. W. *Am. Cryst. Assoc. Abs.* **1985**, *13*, 72.
(13) Adams, W. W.; Grieshop, T.; Helminiak, T.; Hunsaker, M.; O'brien, J. F.; Altieri, M.; Bai, S. J.; Brandt, M.; Fratini, A. V.; Hwang, W.-F.; Price, G. E.; Soloski, E.; Haddock, T.; Krause, S. J.; Lenhert, P. G. AFMAL-TR-86-4011, 1986.
(14) Krause, S. J.; Haddock, T. B.; Vezie, D. L.; Lenhert, P. G.; Hwang, W.-F.; Price, G. E.; Helminiak, T. E.; O'brien, J. F.; Adams, W. W. *Polymer* **1988**, *29*, 1354.
(15) Adams, W. W.; Kumar, S.; Martin, D. C.; Shimamura, K. *Polym. Commun.* **1989**, *30*, 285.
(16) Martin, D. C.; Thomas, E. L. *Macromolecules* **1991**, *24*, 2450.
(17) Fratini, A. V.; Lenhert, P. G.; Resch, T. J.; Adams, W. W. *Mater. Res. Soc. Symp. Proc.* **1989**, *134*, 465.
(18) Jones, M.-C. G.; Martin, D. C. *Macromolecules* **1995**, *28*, 6161.
(19) Chu, S.-G.; Venkatraman, S.; Berry, G. C.; Einaga, Y. *Macromolecules* **1981**, *14*, 939.
(20) Takahashi, Y. *Macromolecules* **1999**, *32*, 4010.
(21) Connolly, J. W.; Dudis, D. S. *Polymer* **1993**, *34*, 1477.
(22) Nelson, D. S.; Soane, D. S. *Polym. Eng. Sci.* **1994**, *34*, 965.
(23) Kitagawa, T.; Yabuki, K. *J. Polym. Sci., Part B: Polym. Phys.* **2000**, *38*, 2901.
(24) Kitagawa, T.; Ishitobi, M.; Yabuki, K. *J. Polym. Sci., Part B: Polym. Phys.* **2000**, *38*, 1605.
(25) Martin, D. C. *Macromolecules* **1992**, *25*, 5171.
(26) Suehiro, K.; Chatani, Y.; Tadokoro, H. *Polym. J.* **1975**, *7*, 352.
(27) Granier, T.; Thomas, E. L.; Karasz, E. *J. Polym. Sci., Part B: Polym. Phys.* **1989**, *27*, 469.
(28) Kitagawa, T.; Murase, H.; Yabuki, K. *J. Polym. Sci., Part B: Polym. Phys.* **1998**, *36*, 39.
(29) Cohen, Y.; Adams, W. W *Polymer* **1996**, *37*, 2767.
(30) Cohen, Y.; Buchner, S.; Zachmann, H. G.; Davidov, D. *Polymer* **1992**, *33*, 3811.
(31) Cohen, Y.; Cohen, E. *Macromolecules* **1995**, *28*, 3631.
(32) Cohen, Y.; Saruyama, Y.; Thomas, E. L. *Macromolecules* **1991**, *24*, 1161.
(33) Bai, S. J.; Hwang, W.-F.; Wiff, D. R.; Price, G. E.; Hunsaker, M. *Bull. Am. Phys. Soc.* **1984**, *29*, 455.
(34) Bai, S. J.; Price, G. E. *Polymer* **1992**, *33*, 2136.
(35) Kumar, S.; Warner, S.; Grubb, D. T.; Adams, W. W. *Polymer* **1994**, *35*, 5408.
(36) Nolan, S. J.; Broomall, C. F.; Bubeck, R. A.; Landes, B. G.; Rudolf, P. R.; Mills, M. J.; Radler, M. J.*Mater. Res. Soc. Symp. Proc.* **1993**, *305*, 111.
(37) Nolan, S. J.; Broomall, C. F.; Bubeck, R. A.; Radler, M. J.; Landes, B. G. *Rev. Sci. Instrum.* **1995**, *66*, 2652.
(38) Ran, S.; Fang, D.; Zong, X.; Hsiao, B. S.; Chu, B.; Cunniff, P. M. *Polymer* **2001**, *42*, 1601.
(39) Gillie, J. K.; Newsham, M. D.; Sen, A.; Bubeck, R. A. *J. Polym. Sci., Part B: Polym. Phys.* **1995**, *33*, 1621.
(40) Donald, A. M.; Windle, A. H. *Liquid Crystalline Polymers*; Cambridge University Press: New York, 1992; p 154.

MA010249G